Joint Path Selection and Resource Allocation in Multi-Hop mmWave-based IAB Systems

Nikita Tafintsev†, Dmitri Moltchanov†, Shu-ping Yeh⋆, Hosein Nikopour⋆, Wei Mao⋆, Oner Orhan⋆, Shilpa Talwar⋆, Mikko Valkama†, and Sergey Andreev†
†Tampere University, Tampere, Finland
⋆Intel Corporation, Santa Clara, CA, USA

***Abstract*—Recently proposed by 3GPP, Integrated Access and Backhaul (IAB) technology promises to deliver a cost-efficient and flexible solution for network densification in 5G/6G systems. Since IAB architecture is based on multi-hop topology and advanced functionalities, such as multi-connectivity transmission and multi-routing, the potential utilization of IAB systems raises an issue of efficient system design. In this paper, we develop an optimization framework capable of jointly selecting transmission paths and allocating radio resources in compliance with half-duplexing and interference constraints. The presented numerical results illustrate that directional mmWave beams employed at the wireless backhaul are essential for capacity boosting, thus allowing to fully exploit the radio resources in self-backhauled systems. We also establish that the multi-hop IAB topology provides advantages in terms of end-to-end user throughput as compared to single-hop systems.**

I. Introduction

Integrated Access and Backhaul (IAB) technology has been recently proposed by 3GPP as a potential solution for network operators to enhance coverage and to densify 5G/6G deployments. Particularly, IAB is considered as a promising approach that provides a flexible wireless backhaul option over 5G New Radio (NR) technology, where only a subset of base stations connects to the fiber core network.

Compared to traditional fiber backhaul networks, wireless IAB architecture allows for deployment flexibility and supports multi-hop operation, thus enabling resilient topology mindful of the network traffic conditions [1]. IAB technology supports both sub-6 GHz and millimeter-wave (mmWave) radios and can operate in standalone (SA) or non-SA (NSA) regime. In practice, IAB is most relevant for mmWave, where backhaul links can leverage a higher amount of spectrum and further benefit from massive beamforming. Also, 3GPP considers IAB networks with both in-band and out-of-band operational modes. In the former, the same spectrum is utilized at both access and backhaul, whereas in the latter, the access and backhaul links use separate frequency bands. The main focus of 3GPP is set on the in-band operational mode, since it allows to efficiently utilize scarce spectrum resources.

In-band IAB operational mode necessarily involves the multiplexing of both access and backhaul traffic. Hence, the radio resources need to be orthogonally divided between the access and the backhaul, either in time, frequency, or space, using centralized or decentralized scheduling coordination. As considered in [1], IAB is expected to rely upon time-division multiplexing (TDM). A TDM network is configured based on time-domain coordination to efficiently multiplex access and backhaul links in both downlink (DL) and uplink (UL) directions. 3GPP prioritizes half-duplex operations, which involve the inability to simultaneously receive and transmit at a single node. Additionally, the advanced IAB capabilities include multi-beam functionality, where separate directional beams are employed for the backhaul links, and multi-connectivity transmission, where several access links are simultaneously maintained for a user equipment (UE). As a result, optimal path selection and radio resource allocation in such systems are crucial for their efficient operation.

The authors in [2] study the problem of path selection and rate allocation in multi-hop self-backhauled mmWave networks. They decompose the problem into path selection and rate allocation sub-problems. Then, the developed framework selects the best paths using reinforcement learning techniques. Similarly, the authors in [3] consider the centralized scheduling and routing problem and investigate the system performance in terms of UE throughput. The authors in [4] study backhaul bandwidth partition strategies in mmWave-capable IAB systems. They propose an analytical framework and investigate various bandwidth partition options. However, those authors focus on the resource split between access and backhaul without considering path selection. In contrast, the authors in [5] study different path selection techniques by disregarding the resource allocation problem. Also, in [6], they evaluate end-to-end performance of IAB systems in terms of the experienced throughput and latency by considering realistic traffic models. With the focus on topology formation in IAB networks, a sequence-based topology formation algorithm is proposed in [7]. The impact of multi-connectivity, multi-beam antennas, and multi-hop configurations on throughput enhancements is quantified in [8]. None of these past studies, however, address joint path selection and resource allocation by simultaneously capturing half-duplexing and interference constraints.

In this paper, path selection and resource allocation in mmWave-based IAB systems are optimized jointly to maximize the end-to-end UE throughput. We address a multi-hop IAB system by accounting for its multi-beam and multi-connectivity capabilities. Specifically, in our framework, the set of paths reflects the network topology, while the resource allocation procedure distributes the radio resources over the set of identified paths for each UE.

The main contributions of this work are as follows:

- We propose an algorithm that accounts for half-duplexing and interference constraints in multi-hop IAB systems. This algorithm allows selecting data transfer paths by employing time-domain coordination, i.e., avoiding simultaneous transmission and reception at a single node, and satisfying the requirement of ancestor-descendant relation between any two IAB-nodes;
- We develop an optimization framework for joint path selection and resource allocation in multi-hop IAB systems. It is shown that where the UE throughput is the primary optimization criterion, a major capacity boost is enabled by multi-beam functionality, while the effect of multi-connectivity is of secondary importance.

The rest of this paper is organized as follows. First, we introduce the system model in Section II. Then, we formulate the joint path selection and resource allocation optimization problem in Section III. Further, we provide numerical results in Section IV. Conclusions are drawn in Section V.

II. System Model

1) Deployment Model: We consider a multi-hop IAB-based heterogeneous system with macro- and micro-layers, where a single IAB-donor at the macro layer supports multiple IAB-nodes randomly distributed in its coverage area by complying with system-level evaluation assumptions as specified by 3GPP in [1], see Fig. 1. We assume that the considered scenario has a constant number of active UEs uniformly distributed in the cell, where each UE generates elastic traffic in UL by following the full-buffer model. In this model, UE data rates vary according to the network conditions and the packet buffers always have data to transmit.

IAB systems utilize Central Unit (CU) and Distributed Unit (DU) split architecture, which enables efficient support of multi-hopping [1]. Specifically, each IAB-node has a Mobile Termination (MT) part used for wireless backhauling toward an upstream IAB-node or IAB-donor. Via the DU, the IAB-node establishes RLC-channels to UEs and to MTs of other downstream IAB-nodes. In the case where an IAB-node is connected via multiple paths, different identifiers in the adaptation layer are to be associated with the paths, thus enabling adaptation layer routing over wireless backhaul topology. Routing on the wireless backhaul links is supported by the adaptation layer, where Backhaul Adaptation Protocol (BAP) is responsible for routing packets from IAB-donor to the target IAB-node and vice versa.

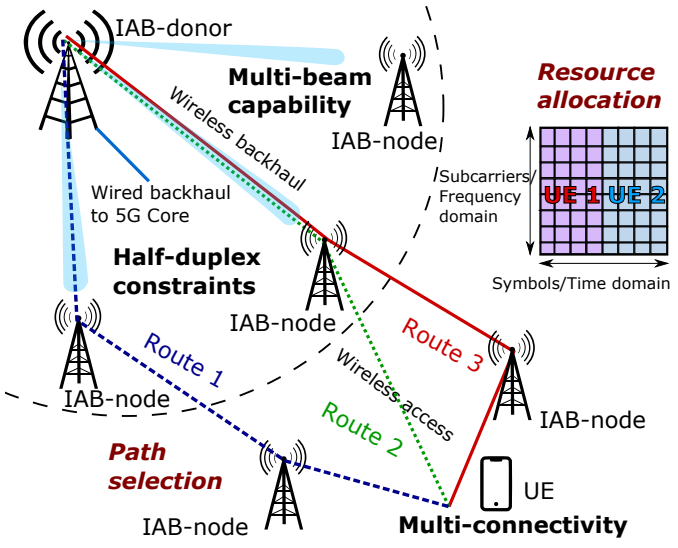

Fig. 1. Multi-hop IAB-based system topology.

We concentrate on studying in-band IAB operational mode, which assumes the utilization of the same frequency band for backhaul and access links and leads to the half-duplexing constraint. The time-domain coordination is required to avoid the full-duplex problem, where transmissions to be received by the MT are severely interfered by DU transmissions. It implies that the IAB-node cannot transmit and receive simultaneously. One of the approaches to avoid intra-node interference is to ensure that the DU and MT transmissions or receptions are separated in the spatial domain, where they operate simultaneously on the same frequency band but within different antenna panels pointing in opposite directions. In this case, one can envision simultaneous DU/MT operation, where the DU and MT are working in different transmission directions. Therefore, an IAB TDM network needs to be configured with a pattern for the time-domain allocation of DL and UL resources [9].

2) Propagation Models: To capture mmWave propagation, we utilize the 3GPP Urban Macro (UMa) channel model for IAB-donor-to-UE and IAB-donor-to-IAB-node interfaces, and Urban Micro (UMi) street canyon channel model for IAB-node-to-UE and IAB-node-to-IAB-node interfaces [10]. The height of UEs carried by pedestrians is assumed to be h_U, while the height of IAB-donor is h_D and the height of IAB-nodes is h_N.

3) Antenna Model: To model antenna array systems for the IAB-donor, IAB-nodes, and UEs, we employ planar uniform rectangular antenna arrays by following the evaluation assumptions in [1]. We consider single- and multi-beam antenna operations at IAB-donor, where the latter is enabled by the use of hybrid/digital beamforming [11]. When the multi-beam regime is considered, the emitted power is assumed to be split equally between the available beams.

4) Metric of Interest: Our main metric of interest is per-UE throughput. Note that this metric heavily depends on the fairness criteria utilized for optimization. In our study, we use a max-min objective function. However, similarly to [12], one may extend it to the case of α-fairness formulation capable of capturing a wide range of fairness criteria, including max-min, proportional fairness, and resource usage maximization.

III. Joint Path Selection and Resource Allocation

In this section, we first formulate the optimization problem. Then, we provide an algorithm for path identification in multi-hop IAB systems under the half-duplex limitation.

A. Problem Formulation

Let M be the number of IAB-nodes in the system having the index $m = 1, 2, \ldots, M$. Also, denote by N the number of UEs in the system. We label the UEs with the indices $n = 1, 2, \ldots, N$. Each UE n is characterized by the achievable user data rate. These data rates are expressed in bits per second (bps) and denoted as

$$d_n,\ n = 1, 2, \ldots, N, \tag{1}$$

which can be determined such that a certain fairness criterion is satisfied.

Each UE n is assigned a set of all the available paths (also named routes) that can carry data traffic. For UE n, the total number of assigned paths is denoted by P_n and they are labeled with index p from the first path to the total number of paths, i.e., $p = 1, 2, \ldots, P_n$. To tie them to a generic UE n, we define paths $\mathcal{P}_{np}, n = 1, 2, \ldots, N, p = 1, 2, \ldots, P_n$. Here, each path is characterized by the links of which the path is composed. We define access links as sets of links for each of the IAB-nodes and the IAB-donor. Specifically, let $\mathcal{A}_0 = \{1, 2, .., U_0\}$ be a set of access links at the IAB-donor that connect to UEs, $\mathcal{A}_m = \{U_{m-1} + 1, U_{m-1} + 2, \ldots, U_m\}$ is a set of access links at the IAB-node m, $m = 1, 2, \ldots, M$. Then, let $\mathcal{A}_{M+1} = \{U_M + 1, U_M + 2, \ldots, U_{M+1}\}$ be a set of backhaul links. Each path $\mathcal{P}_{np}$ is then defined as a set that includes one access link from a certain set $\mathcal{A}_m$ and certain links from the set $\mathcal{A}_{M+1}$ if UE is connected to IAB-node. Alternatively, the path $\mathcal{P}_{np}$ consists of a single link from $\mathcal{A}_0$ if UE is connected to IAB-donor. It is important to note that each path $\mathcal{P}_{np}$ connects the end nodes, i.e., UE and IAB-donor.

In the multi-beam operational mode, separate directional beams are employed for the backhaul links at both IAB-donor and IAB-nodes. In this mode, each backhaul link has a fixed capacity with limited resources. Overall, there are $E = |\mathcal{A}_{M+1}|$ backhaul links, including both IAB-node-to-IAB-donor and IAB-node-to-IAB-node backhaul links, which are indexed as $e = 1, 2, \ldots, E$. We further introduce link-path-incidence variables δ_{enp}, which indicate the link-path relation. Formally, coefficient δ_{enp} is defined for each triple (e, n, p), where $e = 1, 2, \ldots, E$, $n = 1, 2, \ldots, N$, and $p = 1, 2, \ldots, P_n$, which leads to

$$\delta_{enp} = \begin{cases} 1, & \text{if link } e \text{ belongs to path } p \text{ of UE } n, \\ 0, & \text{otherwise.} \end{cases} \tag{2}$$

In our optimization problem, there are two types of variables. First, let

$$x_{np},\ n = 1, 2, \ldots, N,\ p = 1, \ldots, P_n, \tag{3}$$

be continuous variables realizing a part of the demand of the UE n over the path p. These terms, measured in Hz·s, represent the UE resource allocation. Second, we introduce binary variables $u_{np} \in \{0, 1\}$ associated with each of the variables x_{np}. These integer variables are decision binary variables that receive value 1 if the path is selected, or 0 if not.

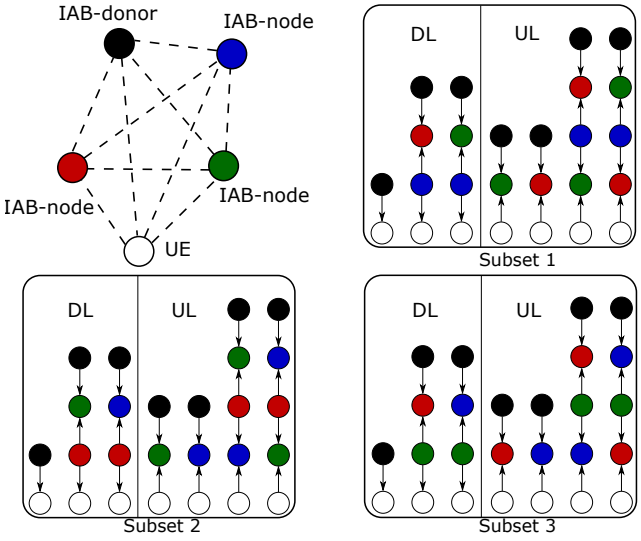

Fig. 2. Illustration of path subsets selection.

First, we determine the achievable UE data rates, which ensure that all the demands are fully realized by using the variables x_{np} and u_{np}. They are defined as

$$d_n = \frac{1}{\Delta} \sum_{p=1}^{P_n} s_{np} x_{np} u_{np}, n = 1, 2, \ldots, N, \tag{4}$$

where Δ is the time slot duration, s_{np} is the spectral efficiency of the access link in the path p. The latter can be calculated as follows

$$s_{np} = \log_2(1 + S_{np}), \tag{5}$$

where S_{np} is the signal-to-interference-plus-noise ratio (SINR) of the access link. The interference component, including inter-cell and self-interference, is approximated by an interference margin [13].

Further, the multi-connectivity constraint is defined as

$$\sum_{p=1}^{P_n} u_{np} \leq k, n = 1, 2, \ldots, N, \tag{6}$$

where k is a predetermined maximum number of paths simultaneously supported by the UEs. This inequality limits the number of access links connecting to the UE n. Note that the constraint (6) assures that only k binary variables associated with a given UE n are equal to 1 and, together with (4), implies that the paths corresponding to the non-zero binary variables carry all the demand volume.

Each IAB-node and IAB-donor has limited time-frequency resources at the access interface. This fact is reflected in the following capacity constraints

$$\sum_{n=1}^{N} \sum_{p=1}^{P_n} \mathbb{1}_{\mathcal{P}_{np} \cap \mathcal{A}_m \neq \emptyset} x_{np} u_{np} \leq B\Delta,\ m = 0, 1, \ldots, M, \tag{7}$$

Algorithm 1 Solving the Path Selection and Resource Allocation Problem in a Multi-Hop IAB System

Input: System parameters

Output: Path selection, resource allocation

Initialization: Enumerate IAB-nodes, UEs, and IAB-donor

1: Construct a graph G connecting the end nodes, i.e., UE and IAB-donor
2: Find all the paths from the given graph G by using, e.g., the depth-first search algorithm and form a list of paths L
3: Assign directions for the links in each path
4: Form S subsets of paths from the list of paths L
5: **for** $s = 1$ to S **do**
6: Perform optimization procedure for the subset s
7: **end for**
8: Compare S subsets according to the metric of interest
9: Select the best subset of paths
10: **return** Path selection, resource allocation

where $\mathbb{1}$ is an indicator function that is defined as

$$\mathbb{1} = \begin{cases} 1, & \text{if } \forall n : \mathcal{P}_{np} \cap \mathcal{A}_m \neq \emptyset, \\ 0, & \text{otherwise}, \end{cases} \tag{8}$$

where B is the system bandwidth. It is assumed that within each time slot, the scheduler can allocate radio resources to meet the needs of all paths, as long as these inequalities are satisfied.

Finally, we introduce the backhaul constraints, which determine link load on e as per the following expression

$$\sum_{n=1}^{N} \sum_{p=1}^{P_n} \delta_{enp} s_{np} x_{np} u_{np} \leq s_e B \Delta, \; e = 1, 2, \ldots, E, \tag{9}$$

where s_e is the spectral efficiency of backhaul link e.

Let us now define the objective function. To derive a solution for max-min fairness, it takes the following form

$$\textbf{maximize} \min\{d_n : n = 1, 2, \ldots, N\}. \tag{10}$$

This objective function can be alternatively expressed by maximizing an additional variable z that is a lower bound for each of the individual variables as

$$\textbf{maximize: } z \tag{11}$$

$$\textbf{subject to: } z \leq \frac{1}{\Delta} \sum_{p=1}^{P_n} s_{np} x_{np} u_{np}, n = 1, 2, \ldots, N. \tag{12}$$

The aforementioned problem is classified as a mixed-integer nonlinear programming (MINLP) problem, known to be $\mathcal{NP}$-complete [14], which can be solved using exact algorithms, such as branch-and-cut or branch-and-bound. Further performance improvements can be achieved by utilizing various relaxation techniques, e.g., local branching or neighborhood search. Approximation approaches, such as simulated annealing or evolutionary algorithms, are also applicable [14]. Note that by assuming predetermined paths, i.e., by avoiding multiplication of $x_{np}u_{np}$, we arrive at a linear programming problem that can be solved in polynomial time. Also, the range extension technique applied to spectral efficiencies can be used to enforce generic α-fairness objective function, while keeping the problem to be of linear programming type [12].

B. Path Identification

The half-duplex constraint does not allow for the utilization of all the available paths simultaneously. Specifically, it limits the number of paths that may be chosen for concurrent transmissions. We now proceed with determining the paths that satisfy the half-duplex constraint. These paths are used as the sets of available paths in the optimization problem that selects the optimal paths for each UE and provides the UE radio resource allocations in the IAB network.

First, we define the set of available routes that can carry data traffic. Initially, each IAB-node can be connected to any IAB-node and IAB-donor (Fig. 2). It is worth noting that each path connects the end nodes, i.e., UE and IAB-donor. Therefore, we utilize single directional access and IAB-donor links, whereas all other links are bidirectional. Note that one has to avoid cycles when counting all the available paths, i.e., a path must comprise a link only once. To perform this procedure, we utilize the depth-first search algorithm and avoid cycles by storing the visited vertices. The output of the algorithm is all possible paths between UE and IAB-donor.

Further, we assign directions, UL or DL, for each of the links in each path. After that, to satisfy the half-duplex constraint, we select the paths, which contain the same receiving and transmitting nodes (i.e., the radio interface at each node should either receive or transmit). Therefore, we divide the set of paths into subsets of paths satisfying half-duplex constraint. This is shown in Fig. 2, where three subsets are identified. Note that 3GPP only specifies either tree or directed acyclic graph (DAG) topology for IAB networks. A DAG topology requires an ancestor-descendant relation between any two IAB-nodes. Hence, an IAB-node cannot be both an ancestor and a descendant of another IAB-node, which further limits the possible routes. The rest of paths in a single subset can be leveraged by the optimization problem. Additionally, UEs can utilize paths in multi-connectivity transmission mode without violating the half-duplex constraint, according to each transmission direction.

The proposed solution algorithm is offered in Algorithm 1. After the overall identification of the subsets, we optimize the system specifically by using each subset of paths. Since the optimization procedure is run individually for a subset of all the available paths, we repeat the optimization process for each subset. In the end, according to the target metric of interest, we compare the subsets and choose the best UE path selections and resource allocations. Once paths are determined, further solution is of polynomial complexity, while the path search itself is $\mathcal{NP}$-hard problem. However, considering that the IAB-donor supports a limited number of IAB-nodes, the overall complexity is low.

TABLE I
DEFAULT SYSTEM PARAMETERS FOR NUMERICAL ASSESSMENT.

Parameter	Value
Cell radius	100 m
Carrier frequency	30 GHz
System bandwidth, B	400 MHz
IAB-donor height, h_D	25 m
IAB-node height, h_N	15 m
UE height, h_U	1.5 m
IAB-donor Tx power	40 dBm
IAB-node Tx power	33 dBm
IAB-donor/IAB-node receiver noise figure	7 dB
UE Tx power	23 dBm
UE receiver noise figure	13 dB
IAB-donor antenna size	16×16
IAB-node antenna size	8×8
UE antenna size	4×4
Number of UEs, N	30 units
Number of IAB-nodes, M	6 units
Interference margin	3 dB
Maximum number of paths for UEs, k	2

IV. NUMERICAL RESULTS

In this section, we apply the developed framework to provide illustrative results. Particularly, we concentrate on the effects of system parameters and advanced IAB functionalities. To solve the MINLP problem, we utilize the advanced process optimizer (APOPT) algorithm in the GEKKO optimization suite [15]. APOPT is an active-set sequential quadratic programming solver that uses the branch-and-bound method and a warm-start approach to speed up successive nonlinear programming solutions. The default system parameters are provided in Table I.

We start by addressing the effect of cell size. To this aim, Fig. 3 shows end-to-end UE throughput as a function of the cell radius for 30 UEs and 3 IAB-nodes under different configurations of the IAB system. As one may observe, for all the considered configurations, an increase in the cell size leads to UE throughput drop. This behavior is explained by degrading channel conditions. Further, an exceptional capacity boost is observed by utilizing multi-beam functionality at IAB-donor, which results in more than 90% improvement in the UE throughput. Contrarily, the use of multi-hop functionality leads to an insignificant increase in the UE throughput across the entire considered range of the cell radii. Finally, the effect of multi-connectivity on throughput is practically marginal. However, multi-connectivity is known to improve reliability and latency [16], [17].

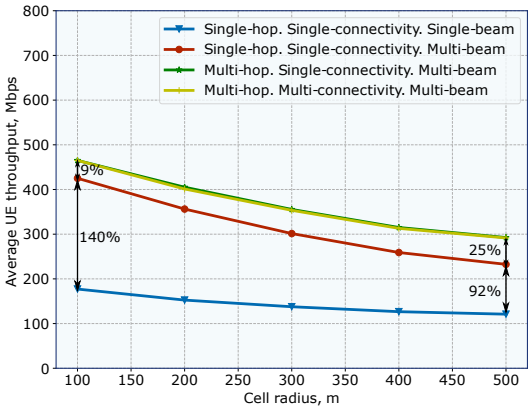

Fig. 3. UE throughput as a function of the cell radius.

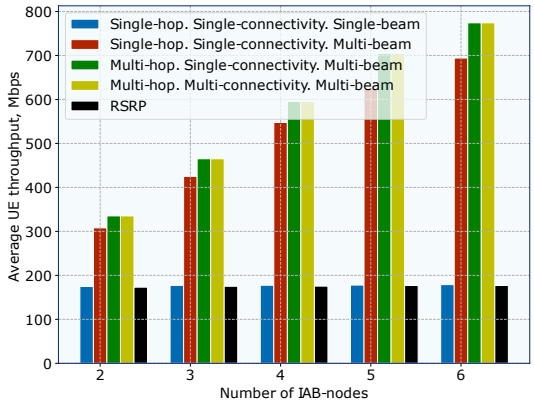

Fig. 4. UE throughput as a function of the number of IAB-nodes.

We now proceed by considering the effect of network densification. Fig. 4 reports end-to-end UE throughput as a function of the number of IAB-nodes for 30 UEs randomly and uniformly distributed in the cell area of 100 m. In addition to different IAB system configurations, we demonstrate UE throughput for RSRP-based operation, where UEs connect to the nearest IAB-node or IAB-donor. First, as one may observe, network densification does not affect the UE throughput in a single-beam regime. The rationale is that the considered system is heavily backhaul-limited. The multi-beam operational mode, however, leads to increased backhaul bandwidth, thus resulting in drastically enhanced UE throughput. Analyzing the presented data, one may notice that multi-hop operation allows for an increase in the UE throughput. However, the associated growth is limited to approximately $5 - 10\%$. The increase of the cell radii can further improve the gains of multi-hop IAB topology.

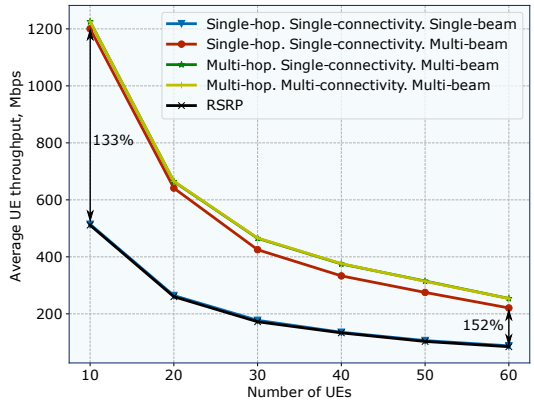

Fig. 5. UE throughput as a function of the number of UEs.

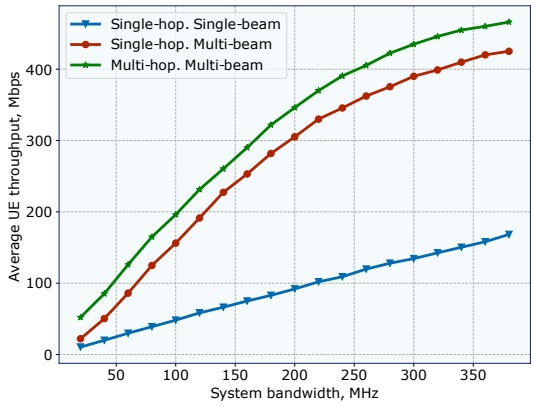

Fig. 6. UE throughput as a function of the system bandwidth.

In Fig. 5, we illustrate the end-to-end UE throughput as a function of the number of UEs for 3 IAB-nodes inside the cell of radius 100 m for all the considered IAB system configurations. Similar to the previous results, the single-beam regime yields the poorest performance. Full utilization of backhaul resources is enabled by the multi-beam, multi-hop operational regime.

Finally, Fig. 6 shows UE throughput as a function of system bandwidth for single- and multi-hop deployments, with and without multi-beam operation. These data further confirm that the use of multi-beam antennas at IAB-donor allows for drastic improvements in UE throughput. On top of this, when multi-hop topology is employed, the gains increase linearly with the available bandwidth. Starting from approximately 200 MHz, the difference between multi-beam and single-beam operation is maintained on a constant level, but still shows more than two times improvement. On the other hand, the gain of utilizing the multi-hop topology is on the order of $5-10\%$ and remains constant for all the considered system bandwidth options.

V. Conclusion

In this paper, the UE throughput optimization problem is investigated by jointly considering path selection and resource allocation in mmWave-based multi-hop IAB systems. The developed approach explicitly accounts for inherent half-duplexing constraints and technological features of IAB setups. The presented numerical results highlight the effects of advanced IAB configurations on the UE throughput.

In particular, we demonstrate that multi-beam functionality is beneficial for capacity boosting in IAB systems, which helps better exploit the radio resources in self-backhauled systems. On the other hand, multi-connectivity is mainly useful for blockage mitigation, but its impact on capacity boosting is limited and thus remains more applicable for latency and reliability enhancements.

Acknowledgment

This work was supported by Intel Corporation, Academy of Finland (projects RADIANT, IDEA-MILL, and SOLID), and JAES Foundation via STREAM project.

References

[1] 3GPP, "Study on integrated access and backhaul (Release 16)," TR 38.874 V16.0.0, 3GPP, Jan. 2019.

[2] T. K. Vu, M. Bennis, M. Debbah, and M. Latva-aho, "Joint path selection and rate allocation framework for 5G self-backhauled mm-wave networks," *IEEE Trans. Wireless Commun.*, vol. 18, no. 4, pp. 2431–2445, 2019.

[3] D. Yuan, H. Lin, J. Widmer, and M. Hollick, "Optimal joint routing and scheduling in millimeter-wave cellular networks," in *IEEE Conf. Comp. Commun.*, pp. 1205–1213, 2018.

[4] C. Saha, M. Afshang, and H. S. Dhillon, "Bandwidth partitioning and downlink analysis in millimeter wave integrated access and backhaul for 5G," *IEEE Trans. Wireless Commun.*, vol. 17, no. 12, pp. 8195–8210, 2018.

[5] M. Polese, M. Giordani, A. Roy, D. Castor, and M. Zorzi, "Distributed path selection strategies for integrated access and backhaul at mmWaves," in *IEEE Glob. Commun. Conf.*, pp. 1–7, 2018.

[6] M. Polese, M. Giordani, A. Roy, S. Goyal, D. Castor, and M. Zorzi, "End-to-end simulation of integrated access and backhaul at mmWaves," in *IEEE Int. Workshop on CAMAD*, pp. 1–7, 2018.

[7] M. Simsek, M. Narasimha, O. Orhan, H. Nikopour, W. Mao, and S. Talwar, "Optimal topology formation and adaptation of integrated access and backhaul networks," *Front. Comms. Net.*, vol. 1, pp. 1–12, 2021.

[8] Y. Sadovaya, D. Moltchanov, W. Mao, O. Orhan, S.-p. Yeh, H. Nikopour, S. Talwar, and S. Andreev, "Integrated access and backhaul in millimeter-wave cellular: Benefits and challenges," *IEEE Commun. Mag.*, vol. 60, no. 9, pp. 81–86, 2022.

[9] E. Dahlman, S. Parkvall, and J. Skold, *5G NR: The next generation wireless access technology*. Academic Press, 2020.

[10] 3GPP, "Study on channel model for frequencies from 0.5 to 100 GHz (Release 17)," TR 38.901 V17.0.0, 3GPP, Mar. 2022.

[11] F. Sohrabi and W. Yu, "Hybrid Analog and Digital Beamforming for mmWave OFDM Large-Scale Antenna Arrays," *IEEE J. Sel. Areas Commun.*, vol. 35, no. 7, pp. 1432–1443, 2017.

[12] M. Gerasimenko, D. Moltchanov, S. Andreev, Y. Koucheryavy, N. Himayat, S.-p. Yeh, and S. Talwar, "Adaptive resource management strategy in practical multi-radio heterogeneous networks," *IEEE Access*, vol. 5, pp. 219–235, 2016.

[13] Y. Sadovaya, D. Moltchanov, H. Nikopour, S.-p. Yeh, W. Mao, O. Orhan, S. Talwar, and S. Andreev, "Self-interference assessment and mitigation in 3GPP IAB deployments," in *IEEE Int. Conf. Commun.*, pp. 1–6, 2021.

[14] M. Pióro and D. Medhi, *Routing, flow, and capacity design in communication and computer networks*. Elsevier, 2004.

[15] L. D. Beal, D. C. Hill, R. A. Martin, and J. D. Hedengren, "GEKKO optimization suite," *Processes*, vol. 6, no. 8, p. 106, 2018.

[16] M. Giordani, M. Mezzavilla, S. Rangan, and M. Zorzi, "Multi-connectivity in 5G mmWave cellular networks," in *2016 Mediterranean Ad Hoc Networking Workshop (Med-Hoc-Net)*, pp. 1–7, 2016.

[17] F. B. Tesema, A. Awada, I. Viering, M. Simsek, and G. P. Fettweis, "Multiconnectivity for mobility robustness in standalone 5G ultra dense networks with intrafrequency cloud radio access," *Wireless Commun. and Mob. Comput.*, 2017.